Journal of Magnetism and Magnetic Materials xxx (2017) xxx–xxx

Contents lists available at ScienceDirect

Journal of Magnetism and Magnetic Materials

journal homepage: www.elsevier.com/locate/jmmm

Research articles

Spin wave propagation in perpendicularly magnetized nm-thick yttrium iron garnet films

Jilei Chen [a,1], Florian Heimbach [a,1], Tao Liu [b], Haiming Yu [a,*], Chuanpu Liu [a,c], Houchen Chang [b], Tobias Stückler [a], Junfeng Hu [a], Lang Zeng [a], Youguang Zhang [a], Zhimin Liao [c], Dapeng Yu [c,d], Weisheng Zhao [a,*], Mingzhong Wu [b]

[a] Fert Beijing Institute, School of Electronic and Information Engineering, BDBC, Beihang University, Xueyuan Road 37, Beijing 100191, China
[b] Department of Physics, Colorado State University, Fort Collins, CO 80523, USA
[c] State Key Laboratory for Mesoscopic Physics and Electron Microscopy Laboratory, School of Physics, Peking University, Beijing 100871, China
[d] Physics Department, Southern University of Science and Technology, Shenzhen 518055, China

ARTICLE INFO

Article history:
Received 9 February 2017
Received in revised form 28 March 2017
Accepted 19 April 2017
Available online xxxx

Keywords:
Magnonics
Spin waves
Antenna design
Yttrium iron garnet

ABSTRACT

Magnonics offers a new way for information transport that uses spin waves (SWs) and is free of charge currents. Unlike Damon-Eshbach SWs, the magneto-static forward volume SWs offer the reciprocity configuration suitable for SW logic devices with low power consumption. Here, we study forward volume SW propagation in yttrium iron garnet (YIG) thin films with an ultra-low damping constant $\alpha = 8 \times 10^{-5}$. We design different integrated microwave antenna with different *k*-vector excitation distributions on YIG thin films. Using a vector network analyzer, we measured SW transmission with the films magnetized in perpendicular orientation. Based on the experimental results, we extract the group velocity as well as the dispersion relation of SWs and directly compare the power efficiency of SW propagation in YIG using coplanar waveguide and micro stripline for SW excitation and detection.

1. Introduction

Spin waves (SWs) offer a promising new way to transport information without involving charge currents. This property could lead to a new paradigm in the area of computing, allowing to create smaller low-power devices compared to common CMOS-technology [1–8]. An essential part in the development of such circuits is the ability to locally control the SW amplitude. This can be achieved by utilizing interference of SWs due to the control of the SW phase [9–11]. A suitable material for this purpose is yttrium iron garnet (YIG). It offers an ultra-low magnetic damping [12–16], and therefore, a relative long decay length is expected.

Beside the material for SW propagation, the magnetic configuration of the system is also essential. For an in-plane magnetization, the propagation direction of SWs relative to the magnetization direction determines the type of the SW [17–19]. As a result of a static magnetization, the dispersion relation as well as the excitation strength depend on the SW direction. On the contrary, the out-of-plane configuration, leading to the magneto-static forward volume mode (MSFVM), offers a strong SW excitation strength with the possibility to send SWs in arbitrary directions and avoid non-reciprocity effects in SW interferometer compared to the Damon-Eshbach SWs [20–22]. Magnetic simulations has proven that the out-of-plane magnetized majority gate can overcome the limitation of anisotropic in-plane magnetized majority gates due to the high spin-wave transmission [23], which makes MSFVM SWs with the perpendicularly magnetized configuration suitable for SW logic devices free of non-reciprocity effects.

Schwarze et al. studied the MSFVM SWs in Permalloy based magnetic cystals and Vlaminck et al. discovered current-induced MSFVM SW doppler shifts in Permalloy thin films [24,25]. There are also some studies of MSFVM SW in bulk YIG [20,26]. However, few studies have been conducted on MSFVM SW in nm-thick ultra low damping YIG films which are more suitable for the preparation of nano-structures which are desirable for in the creation of small logic circuits.

In the following we use an all electrical FMR measurement technique, utilizing coplanar waveguides and planar micro striplines to determine the properties of MSFVM SWs in a YIG thin film.

* Corresponding authors.
E-mail addresses: haiming.yu@buaa.edu.cn (H. Yu), weisheng.zhao@buaa.edu.cn (W. Zhao).
[1] These authors contributed equally to this work.

http://dx.doi.org/10.1016/j.jmmm.2017.04.045
0304-8853/

2. Device Fabrication

Fig. 1 illustrates the basic information of our experiment. The base was a 20-nm-thick YIG film grown on a gadolinium gallium garnet (GGG) substrate by sputtering [27,12]. Using optical lithography and reactive-ion etching, a waveguide (width 90 μm, length 250 μm, thickness $t = 20$ nm) was created. To avoid interference with reflected SWs, the mesa is tapered at both ends.

To excite and detect SWs in the material, two kinds of antenna have been fabricated. A so called coplanar wave guide (CPW) [28] (line width 2 μm, edge to edge separation between the ground and signal lines 1.6 μm) and a micro stripline (MSL) (width 1 μm)[29]. It is important to note that the MSL employed in this work has no ground plane. Instead one side of the antenna is connected to an RF-signal while the other side of the MSL is directly connected to the ground potential. In both cases, the CPW and the MSL, we fabricate two identical antennas with a distance s of 30 μm between signal lines of the CPWs or between the MSLs respectively. By connecting this antennas via microwave probes to a vector network analyzer (VNA) an RF-current can be sent through the antennas. The resulting RF-magnetic field leads to the excitation of SWs which on the other hand create a changing magnetic flux. The changing flux then induces an RF-current in the antennas and can thereby be detected by the VNA. The k-vectors of the excited SWs depend on the design of the antennas and can be obtained by a Fourier transformation of whose spatial magnetic excitation field distribution. For the CPW an electromagnetic simulation performed by Schwarze [30] has been used to determine the spatial distribution [17]. In case of the MSL antenna the field was estimated by making the following assumptions. The out-of-plane components of the excitation field can be neglected and we assume a uniform in-plane field component underneath the antenna with a spatial extent equivalent to the width of the stripline. While this is a very rough approximation, the electromagnetic simulation on CPWs showed that it is justified to use this kind of approach [30]. The resulting k-vector distribution for the MSL is illustrated in Fig. 4(b). Due to the width of the prominent maxima the SW excitation and detection can cover a broad range of different k-vectors.

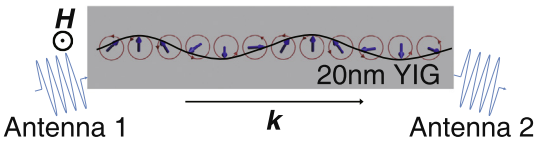

Fig. 1. Schematic of magneto-static forward volume SW propagating in a 20 nm-thick YIG thin film.

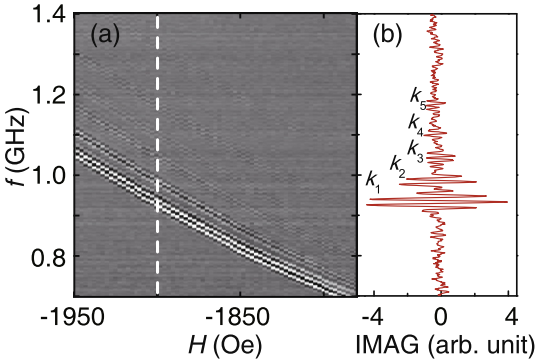

Fig. 2. (a) Gray-scale plot of SW propagation data S_{12}obtained from CPW measurements (b) SW spectrum (S_{12}) at an out-of-plane field of H = −1900 Oe, extracted from the vertical dotted line in (a). The spectra are extracted from the imaginary part of the (S_{12}) parameter of VNA measurement.

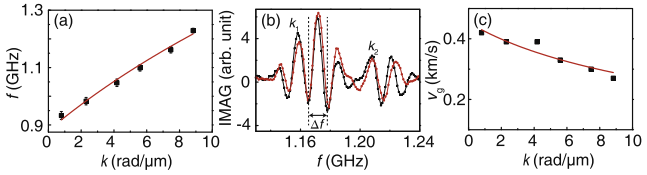

Fig. 3. (a) Experimentally observed dispersion relation at H = −1900 Oe. The red curve is the numerical fit. (b) SW spectra of k_1 and k_2 modes extracted from S_{12} (red circles) and S_{12}(black squares) transmission data from a CPW measurement at H = −1990 Oe. Δf is shown in order to calculate the group velocity. (c) Group velocity of MSFVM SWs with different vectors k at H = −1900 Oe. The red curve shows a numerical fit.

3. Results and discussion

An example of the results of the measurements on the CPW sample can be seen in Fig. 2. It displays the imaginary part of the measured S-parameter S_{12} which describes the signal of a SW generated in antenna 2 and detected in antenna 1 (transmission measurements). The external magnetic field H was applied in the out-of-plane direction (see Fig. 1) and changed from −2000 Oe to 2000 Oe. After an arc-like region the excitation frequency is rising with the absolute value of the applied external field. Additional to the strong main mode, this region also displays several other weaker modes at higher frequencies (see Fig. 2(a)) exhibiting the same general behavior. All these modes, including the main mode, display an oscillation of the signal strength, indicated by the change of white and black in the gray-scale plot. These oscillations can also be seen in the line-plots, as shown in Fig. 2 (b). Similar results are obtained by the measurements with the MSLs. We also observe a region with an arc like mode at lower absolute magnetic field values and a region were the resonance frequency of the mode is increasing with the absolute field value. The MSL transport measurements also display the same oscillating behavior observed in the CPW data. However, while in the CPW measurements we detect several separated modes the MSL measurements exhibits one continuous mode covering a relative large frequency range (see Fig. 4).

The main difference between the CPW and the MSL measurements is the width and the number of observed SW modes (see Figs. 2 and 4). We attribute this to the diverse excitation spectra for the CPW (see [17] and 4(b)) and the MSL (see Fig. 4(b)). Each mode appearing the in CPW measurements can be assigned to a maximum in the excitation profile of the CPW. While the excitation spectrum of the MSL also displays maxima next to most prominent one, those strengths are relative small and as a result only the strongest mode can be observed in the actual measurements.

The two different regions of the measurements can be explained by the magnetization behavior of the YIG film. Without an external field, the magnetization of the YIG is pointing in an arbitrary in-plane direction due to the shape anisotropy of the film. At a saturation field around H = 1700 Oe or stronger fields, the magnetization is pointing out-of-plane in the external field direction and we observe MSFVM SWs. Beside the out-of-plane field, the magnet used in the measurement system also produces a small in-plane component. At higher fields where the influence of the in-plane component is small compared to the out-of-plane component, we can observe a quasi-linear frequency dependence as predicted by the theoretical model for MSFVM SWs [31]

Please cite this article in press as: J. Chen et al., Spin wave propagation in perpendicularly magnetized nm-thick yttrium iron garnet films, Journal of Magnetism and Magnetic Materials (2017), http://dx.doi.org/10.1016/j.jmmm.2017.04.045

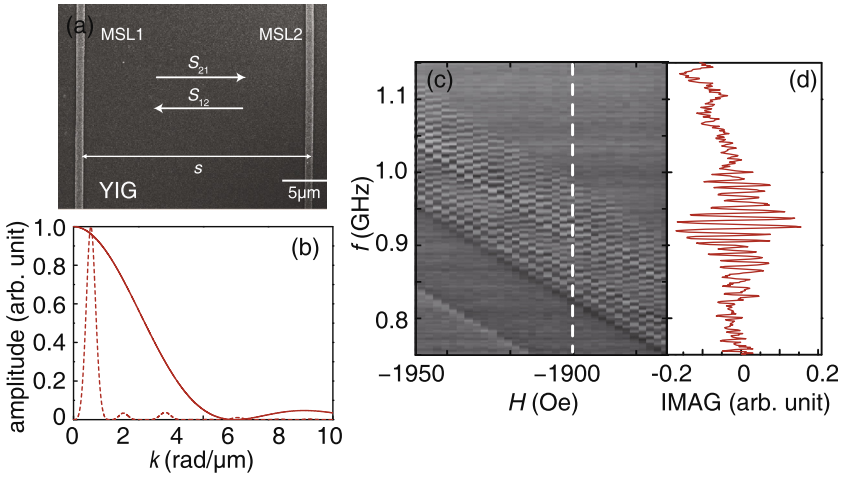

Fig. 4. (a) Scanning electron microscopic image of two MSLs fabricated on a YIG thin film. The distance s between two MSLs is 30 μm. (b) Normalized excitation spectra I(k) obtained by Fourier transformation of an approximated (MSL), and simulated (CPW) excitation field. (c) Gray-scale plot of SW propagation data (S_{12}) obtained from MSL measurements. (d) SW spectrum (S_{12}) at an out-of-plane field of H = −1900 Oe, extracted from the vertical dotted line in (c).

$$\omega_{\mathrm{MSFVW}}^2 = \omega_{\mathrm{H}}\left[\omega_{\mathrm{H}} + \omega_{\mathrm{M}}\left(1 - \frac{1 - e^{-k_{\parallel}t}}{k_{\parallel}t}\right)\right]. \quad (1)$$

with $\omega_{\mathrm{M}} = \gamma\mu_0 M_{\mathrm{S}}, \omega_{\mathrm{H}} = \gamma\mu_0(H_{\mathrm{ext}} - M_{\mathrm{S}})$ and $k_{\parallel}$ as the in-plane k-vector. γ is the absolute gyromagnetic ratio. It is necessary to note that this mode does not depend on the direction of the in-plane wave vector $k_{\parallel}$. This behavior can be also observed in the actual experiment. The SWs represented in the S_{12} and S_{12} measurements have opposite propagation directions. A comparison between the amplitude of these two signals reveals almost no discrepancies (see Fig. 3(b)), which shows the expected reciprocal behavior of the MSFVM spin waves which is different from the DE mode [17]. The small difference between the $S_{12}$and S_{12} spectra may result from the already mention small in-plane field component which may cause a little deviation of the measured data.

The observed dispersion relation is displayed in Fig. 3 (a). By extracting the SW resonance frequencies from the CPW measurement at the different excited k-vectors and using Eq. (1), we can fit the MSFVM SW dispersion relation and obtain a saturation magnetization of $M_{\mathrm{S}} = 1741 \pm 13$ Oe which is in good agreement with the expected value [31].

At resonance condition the imaginary part of the signal shows an oscillating behavior. By analyzing the line-plot at fixed external magnetic fields we extracted the periodicity Δf of the oscillations which can be used to determine the propagation velocity of the SW by utilizing [32,33]

$$v_{\mathrm{g}} \approx \frac{2\pi\Delta f}{2\pi/s} = \Delta f \cdot s. \quad (2)$$

Due to the design of the CPWs, we do not only excite SWs at a certain k-vector but we are exciting wave vectors around multiple maxima. As we can see in the measurements, several of these maxima are strong enough to be observed. The dependence of the group velocity on the k-vector is displayed in Fig. 3(c). The SW group velocity decreases as the k-vector increases which can be understood by analyzing the expected dispersion relation of MSFVM SWs. The fitting curve of the SW group velocity displayed in Fig. 3 (c) was obtained by taking the derivative of (1) [34].

By comparing the SW excitation in CPW measurements with the excitation in the MSL measurements we note that although the MSL excites a broader SW spectrum, the excitation strength is weaker compared to the CPW (around 38%). While the design of the CPWs is chosen to match its impedance to the measurement system, this is not the case for the MSLs. Therefore, we can assume that a part of the power, sent from the VNA to the sample, gets reflected at the MSL before it can excite SWs in the YIG film. As a result of the smaller SW excitation, naturally the signals of the detected SWs are also decreased. The choice of the optimal kind of antenna entirely depends on the application. In some cases it is beneficial to excite and detect k-vectors over a broad range while in some cases it has an advantage to excite only specific k-vectors. There are also applications which profit from a combination of CPW and MSL.

4. Conclusion

In conclusion, we have studied MSFVM SWs in nm-thick YIG films when magnetization is saturated out of plane. Several high order wavevector excitation has been observed and spin wave dispersion relation is extracted from experimental data.The group velocities are estimated to be around 0.4 km/s. The propagation of MSFVM SWs is found to be almost reciprocal, which is ideal to be used in spin wave interference for SW logic devices. Different microwave anntennas have been used to study MSFVM SWs, namely CPWs and MSLs. CPWs excite several wavevector starting from about 0.9 rad/μm up to 8.8 rad/μm, whereas MSLs excite rather broad wavevector distribution. However, while the SW properties are advantageous, the relative large out-of-plane field which is required to produce the MSFVM SW might be a challenge in small electric device. We expect a further optimized film with perpendicular magnetic anisotropy will allow MSFVM SW propagation at even zero applied field.

Acknowledgement

We wish to acknowledge the support by National Nature Science Foundation of China under Grant Nos. 11674020, 11444005, youth 1000 talent program, 111 talent program B16001 and Ministry of Science and Technology of China MOST No. 2016YFA0300802. The growth of YIG thin films was supported by the SHINES, an Energy Frontier Research Center funded by the U.S. Department of Energy, Office of Science, Basic Energy Sciences under Award SC0012670. The characterization of YIG thin films was supported by the U. S. National Science Foundation under Award EFMA-1641989.

Please cite this article in press as: J. Chen et al., Spin wave propagation in perpendicularly magnetized nm-thick yttrium iron garnet films, Journal of Magnetism and Magnetic Materials (2017), http://dx.doi.org/10.1016/j.jmmm.2017.04.045

References

[1] A.V. Chumak, V.I. Vasyuchka, A.A. Serga, B. Hillebrands, Magnon spintronics, Nat. Phys. 11 (2015) 453–461, http://dx.doi.org/10.1038/nphys3347.
[2] K. Vogt, F. Fradin, J. Pearson, T. Sebastian, S. Bader, B. Hillebrands, A. Hoffmann, H. Schultheiss, Realization of a spin-wave multiplexer, Nat. Commun. 5 (2014) 1–5, http://dx.doi.org/10.1038/ncomms4727.
[3] A.V. Chumak, A.A. Serga, B. Hillebrands, Magnon transistor for all-magnon data processing, Nat. Commun. 5 (2014) 4700, http://dx.doi.org/10.1038/ncomms5700.
[4] D. Grundler, Spintronics: nanomagnonics around the corner, Nat. Nanotech. (2016) 1–2, http://dx.doi.org/10.1038/nnano.2016.16.
[5] A. Khitun, K.L. Wang, Nano scale computational architectures with spin wave bus, Superlattices Microstruct. 38 (2005) 184–200, http://dx.doi.org/10.1016/j.spmi.2005.07.001.
[6] A. Khitun, D.E. Nikonov, M. Bao, K. Galatsis, K.L. Wang, Efficiency of spin-wave bus for information transmission, IEEE Trans. Electron Devices 54 (2007) 3418–3421, http://dx.doi.org/10.1109/TED.2007.908898.
[7] J. Lan, W. Yu, R. Wu, J. Xiao, Spin-wave diode, Phys. Rev. X 5 (2015) 041049, http://dx.doi.org/10.1103/PhysRevX.5.041049.
[8] S.B. von Gamm, A. Papp, E. Egel, C. Meier, C. Yilmaz, L. Hei, W. Porod, G. Csaba, Design of on-chip readout circuitry for spin-wave devices, IEEE Magn. Lett. 9 (2017) 3100804, http://dx.doi.org/10.1063/1.4973497.
[9] R. Hertel, W. Wulfhekel, J. Kirschner, Domain-wall induced phase shifts in spin waves, Phys. Rev. Lett. 93 (2004) 257202, http://dx.doi.org/10.1103/PhysRevLett. 93.257202.
[10] F.J. Buijnsters, Y. Ferreiros, A. Fasolino, M.I. Katsnelson, Chirality-dependent transmission of spin waves through domain walls, Phys. Rev. Lett. 116 (2016) 1–5, http://dx.doi.org/10.1103/PhysRevLett. 116.147204.
[11] A. Khitun, M. Bao, K.L. Wang, Magnonic logic circuits, J. Phys. D: Appl. Phys. 43 (2010) 264005, http://dx.doi.org/10.1088/0022-3727/43/26/264005.
[12] H. Chang, P. Li, W. Zhang, T. Liu, A. Hoffmann, L. Deng, M. Wu, Nanometer-thick yttrium iron garnet films with extremely low damping, IEEE Magn. Lett. 5 (2014) 6700, http://dx.doi.org/10.1109/LMAG.2014.2350958.
[13] H. Yu, O. d' Allivy Kelly, V. Cros, R. Bernard, P. Bortolotti, A. Anane, F. Brandl, F. Heimbach, D. Grundler, Approaching soft x-ray wavelengths in nanomagnet-based microwave technology, Nat. Commun. 7 (2016) 11255, http://dx.doi.org/10.1038/ncomms11255.
[14] M.B. Jungfleisch, W. Zhang, W. Jiang, H. Chang, J. Sklenar, S.M. Wu, J.E. Pearson, A. Bhattacharya, J.B. Ketterson, M. Wu, A. Hoffmann, Spin waves in micro-structured yttrium iron garnet nanometer-thick films, J. Appl. Phys. 117 (2015) 17, http://dx.doi.org/10.1063/1.4916027.
[15] M.B. Jungfleisch, W. Zhang, J. Sklenar, J. Ding, W. Jiang, H. Chang, F.Y. Fradin, J.E. Pearson, J.B. Ketterson, V. Novosad, M. Wu, A. Hoffmann, Large spin-wave bullet in a ferrimagnetic insulator driven by the spin hall effect, Phys. Rev. Lett. 116 (2016) 1–6, http://dx.doi.org/10.1103/PhysRevLett. 116.057601.
[16] M. Evelt, V.E. Demidov, V. Bessonov, S.O. Demokritov, J.L. Prieto, M. Munoz, J. Ben Youssef, V.V. Naletov, G. De Loubens, O. Klein, M. Collet, K. Garcia-Hernandez, P. Bortolotti, V. Cros, A. Anane, High-efficiency control of spin-wave propagation in ultra-thin yttrium iron garnet by the spin-orbit torque, Appl. Phys. Lett. 108 (2016) 172406, http://dx.doi.org/10.1063/1.4948252.
[17] H. Yu, O. d' Allivy Kelly, V. Cros, R. Bernard, P. Bortolotti, A. Anane, F. Brandl, R. Huber, I. Stasinopoulos, D. Grundler, Magnetic thin-film insulator with ultra-low spin wave damping for coherent nanomagnonics, Sci. Rep. 4 (2014) 6848, http://dx.doi.org/10.1038/srep06848.
[18] S.O. Demokritov, B. Hillebrands, A.N. Slavin, Brillouin light scattering studies of confined spin waves: linear and nonlinear confinement, Phys. Rep. 348 (2001) 453–461, http://dx.doi.org/10.1016/S0370-1573(00)00116-2.
[19] S. Tacchi, G. Gubbiotti, M. Madami, G. Carlotti, Brillouin light scattering studies of 2D magnonic crystals, J. Phys.: Condens. Matter 29 (2016) 073001, http://dx.doi.org/10.1088/1361-648X/29/7/073001.
[20] N. Kanazawa, T. Goto, K. Sekiguchi, A.B. Granovsky, C.A. Ross, H. Takagi, Y. Nakamura, M. Inoue, Demonstration of a robust magnonic spin wave interferometer, Sci. Rep. 6 (2016) 30268, http://dx.doi.org/10.1038/srep30268.
[21] O. Rousseau, B. Rana, R. Anami, M. Yamada, K. Miura, S. Ogawa, Y. Otani, Realization of a micrometre-scale spin-wave interferometer, Sci. Rep. 5 (2015) 9873, http://dx.doi.org/10.1038/srep09873.
[22] M. Balinskiy, B. Mongolov, D. Gutierrez, H. Chiang, A. Slavin, A. Khitun, Perpendicularly magnetized yig-film resonators and waveguides with high operating power, AIP Adv. 7 (2017) 056612, http://dx.doi.org/10.1063/1.4973497.
[23] S. Klingler, P. Pirro, T. Brächer, B. Leven, B. Hillebrands, A.V. Chumak, Spin-wave logic devices based on isotropic forward volume magnetostatic waves, Appl. Phys. Lett. 106 (2015) 212406, http://dx.doi.org/10.1063/1.4921850.
[24] T. Schwarze, R. Huber, G. Duerr, D. Grundler, Complete band gaps for magnetostatic forward volume waves in a two-dimensional magnonic crystal, Phys. Rev. B 85 (2012) 1–5, http://dx.doi.org/10.1103/PhysRevB.85.134448.
[25] V. Vlaminck, M. Bailleul, Current-induced spin-wave doppler shift, Science 322 (2008) 410–413, http://dx.doi.org/10.1126/science.1162843.
[26] A.B. Ustinov, B.A. Kalinikos, E. Lähderanta, Nonlinear phase shifters based on forward volume spin waves, J. Appl. Phys. 113 (2013) 1–4, http://dx.doi.org/10.1063/1.4795165.
[27] T. Liu, H. Chang, V. Vlaminck, Y. Sun, M. Kabatek, A. Hoffmann, L. Deng, M. Wu, Ferromagnetic resonance of sputtered yttrium iron garnet nanometer films, J. Appl. Phys. 115 (2014) 87–90, http://dx.doi.org/10.1063/1.4852135.
[28] C.P. Wen, Coplanar waveguide: a surface strip transmission line suitable for nonreciprocal gyromagnetic device applications, IEEE Trans. Microwave Theory Tech. 17 (12) (1969) 1087–1090, http://dx.doi.org/10.1109/TMTT.1969.1127105.
[29] F. Ciubotaru, T. Devolder, M. Manfrini, C. Adelmann, I.P. Radu, All electrical propagating spin wave spectroscopy with broadband wavevector capability, Appl. Phys. Lett. 109 (2016) 1–6, http://dx.doi.org/10.1063/1.4955030.
[30] T. Schwarze, Spin waves in 2d and 3d magnonic crystals: From nanostructured ferromagnetic materials to chiral helimagnets, Ph.D. thesis, TECHNISCHE UNIVERSITÄT MÜNCHEN Lehrstuhl für Physik funktionaler Schichtsysteme, E10, 2013.
[31] A. Prabhakar, D.D. Stancil, Spin Waves Theory and Applications, Springer (2009), http://dx.doi.org/10.1007/978-0-387-77865-5.
[32] H. Yu, R. Huber, T. Schwarze, F. Brandl, T. Rapp, P. Berberich, G. Duerr, D. Grundler, High propagating velocity of spin waves and temperature dependent damping in a cofeb thin film, Appl. Phys. Lett. 100 (26) (2012) 1–4, http://dx.doi.org/10.1063/1.4731273.
[33] S. Neusser, G. Duerr, H.G. Bauer, S. Tacchi, M. Madami, G. Woltersdorf, G. Gubbiotti, C.H. Back, D. Grundler, Anisotropic propagation and damping of spin waves in a nanopatterned antidot lattice, Phys. Rev. Lett. 105 (2010) 1–4, http://dx.doi.org/10.1103/PhysRevLett. 105.067208.
[34] B.A. Kalinikos, A.N. Slavin, Theory of dipole-exchange spin wave spectrum for ferromagnetic films with mixed exchange boundary conditions, J. Phys. C: Solid State Phys. 19 (1986) 7013–7033, http://dx.doi.org/10.1088/0022-3719/19/35/014.

Please cite this article in press as: J. Chen et al., Spin wave propagation in perpendicularly magnetized nm-thick yttrium iron garnet films, Journal of Magnetism and Magnetic Materials (2017), http://dx.doi.org/10.1016/j.jmmm.2017.04.045